



A combined molecular dynamics/micromechanics/finite element approach for multiscale constitutive modeling of nanocomposites with interface effects

B. J. Yang, H. Shin, H. K. Lee, and H. Kim

Citation: [Applied Physics Letters](#) **103**, 241903 (2013); doi: 10.1063/1.4819383

View online: <http://dx.doi.org/10.1063/1.4819383>

View Table of Contents: <http://scitation.aip.org/content/aip/journal/apl/103/24?ver=pdfcov>

Published by the [AIP Publishing](#)



MULTIPHYSICS SIMULATION

FREE Multiphysics Simulation e-Magazine

DOWNLOAD TODAY >>

COMSOL

The advertisement features a dark orange background. On the left is a thumbnail of the 'Multiphysics Simulation' e-magazine cover, which shows a computer monitor displaying a simulation of a mechanical part. The cover text includes 'MULTIPHYSICS SIMULATION', 'SPECTRUM', and 'SIMULATION ADVANCES DESIGN AT ABB PAGE 20'. To the right of the thumbnail, the text 'FREE Multiphysics Simulation e-Magazine' is written in a large, white, sans-serif font. Below this text is a dark grey button with the white text 'DOWNLOAD TODAY >>'. In the bottom right corner, the COMSOL logo is displayed, consisting of a small square icon followed by the word 'COMSOL' in a white, sans-serif font.

A combined molecular dynamics/micromechanics/finite element approach for multiscale constitutive modeling of nanocomposites with interface effects

B. J. Yang,¹ H. Shin,² H. K. Lee,¹ and H. Kim^{2,a)}

¹Department of Civil and Environmental Engineering, Korea Advanced Institute of Science and Technology (KAIST), 291 Daehak-ro, Yuseong-gu, Daejeon 305-701, South Korea

²Graduate School of Energy Environment Water Sustainability (EEWS), Korea Advanced Institute of Science and Technology (KAIST), 291 Daehak-ro, Yuseong-gu, Daejeon 305-701, South Korea

(Received 20 June 2013; accepted 9 August 2013; published online 10 December 2013)

We introduce a multiscale framework based on molecular dynamic (MD) simulation, micromechanics, and finite element method (FEM). A micromechanical model, which considers influences of the interface properties, nanoparticle (NP) size, and microcracks, is developed. Then, we perform MD simulations to characterize the mechanical properties of the nanocomposite system (silica/nylon 6) with varying volume fraction and size of NPs. By comparing the MD with micromechanics results, intrinsic physical properties at interfacial region are derived. Finally, we implement the developed model in the FEM code with the derived interfacial parameters, and predict the mechanical behavior of the nanocomposite at the macroscopic scale. © 2013 AIP Publishing LLC. [<http://dx.doi.org/10.1063/1.4819383>]

Nanocomposites have recently been used in the field of composite materials due to their unique mechanical, electrical, and thermal properties.^{1,2} Nanoparticle (NP)-reinforced polymeric composites, a broad category of nanocomposite materials, offer high tensile strength even with low reinforcement concentrations and have become attractive candidate materials for many applications.³ However, the changes in and complexity of polymer properties with the addition of NPs are poorly understood, especially due to the lack of technologies bridging nano- and micro-systems. Whereas the enhanced features are primarily derived from nanoscale fillers, different interfacial characteristics between the matrix and nanoscale inclusions can arise, which restrict precise predictions of the overall behavior of nanocomposites. Understanding the nature of the interfacial properties and physical responses of nanoparticulate composites is therefore essential to the design and implementation of NP-reinforced polymeric systems in real applications.

To investigate the interfacial characteristics of nanocomposite materials, the molecular dynamics (MD) simulation method would be ideal because it can describe the full atomistic nature at the heterogeneous interface between NP and polymeric systems with little empiricism. However, the relatively high computational cost of atomistic MD simulation practically limits its direct application in predicting meso- or macro-scopic material properties, thus requiring micromechanics-based analytical models and/or numerical finite element method (FEM) simulations. However, recent experimental studies have shown that classical composite theory cannot account for the mechanical behavior of nanocomposites:⁴ a decrease in the modulus of nanocomposites is observed in experiments with an increase in the stiffness of NPs,^{5,6} which is inconsistent with the theory that smaller par-

ticle fillers are expected to improve the overall mechanical properties of composites.

Therefore, in this study, we develop a size dependent micromechanical constitutive model in which interface effects are taken into account by introducing model parameters, namely the interface moduli. In this constitutive model, we also note that a continuum damage model of microcracks is incorporated for a realistic assessment of nanocomposites under external loading. Then, we further compare our analytical micromechanics-based results with full atomistic MD simulation results obtained for silica/nylon 6 nanocomposite systems from which the interfacial parameters are identified. We implement the developed constitutive model in the FEM code ABAQUS to solve the boundary condition problem, and the mechanical properties of silica/nylon 6 nanocomposite systems are predicted using the implemented model. The calculated results are in good agreement in the elastic range with the experimental results obtained for silica/nylon 6 nanocomposites. This agreement demonstrates that the presented multiscale simulation approach based on the developed micromechanics theory is effective in predicting the mechanical behavior of NP-reinforced composites.

We first consider a three-phase nanocomposite consisting of a matrix (phase 0) and nanoscale spheres (phase 1) randomly dispersed throughout the matrix.⁷ It is assumed that the nanocomposite experiences the formation of microcracks with an increase in the external tensile load or deformation, which are separately treated as penny-shaped voids in the composites (phase 2). It should be noted that the present micromechanics-based model is to predict the effective constitutive equation of the nanocomposites, and thus it is available only within an elastic range. This is the intrinsic limitation of the proposed model where the modeling of yield strength and plastic behavior is deficient. In micromechanics-based approaches, the effective stiffness tensor C_* for multi-phase nanocomposites ($q = 0, 1, 2$) can be expressed as follows:^{8,9}

^{a)}Electronic mail: linus16@kaist.ac.kr

$$\mathbf{C}_* = \mathbf{C}_0 \cdot \left[\mathbf{I} + \sum_{q=0}^2 \left\{ \left[\mathbf{I} - \phi_q \mathbf{S}_q \cdot (\mathbf{A}_q + \mathbf{S}_q)^{-1} \right]^{-1} \right\} \right], \quad (1)$$

where $\mathbf{A}_q \equiv (\mathbf{C}_q - \mathbf{C}_0)^{-1} \cdot \mathbf{C}_0$; \mathbf{C}_q is the stiffness tensor of the q -phase, and \mathbf{I} is the fourth-order identity tensor; ϕ_q and \mathbf{S}_q represent the volume fraction and the interior-point Eshelby tensor for the q -phase, respectively.

In Eq. (1), \mathbf{S}_1 is the ensemble-averaged Eshelby tensor for nano-inhomogeneity with interface effects,⁸ which is expressed as¹⁰

$$\mathbf{S}_1 = S^{(1)} \delta_{ij} \delta_{kl} + S^{(2)} (\delta_{ik} \delta_{jl} + \delta_{il} \delta_{jk}) \quad (2)$$

in which

$$S^{(1)} = F_3 - F_2 - \frac{21F_1}{5}, \quad S^{(2)} = \frac{1}{2} + \frac{3F_2}{2} + \frac{63F_1}{10} \quad (3)$$

with

$$F_1 = \frac{2\Gamma_1(4 - 5\nu_0)(\kappa_s^r + 2\mu_s^r)}{3\eta_{11}}, \quad F_2 = \frac{\eta_{12}}{3\eta_{11}} \quad (4)$$

$$F_3 = -\frac{(1 - 2\nu_0)(2 + \kappa_s^r)}{3[\Gamma_1(1 + \nu_1) + (1 - 2\nu_1)(2 + \kappa_s^r)]}, \quad (5)$$

where $\Gamma_1 = \mu_1/\mu_0$; μ_q is the shear modulus of the q -phase and η_{1i} ($i = 1, 2$) is given in Yang *et al.*⁸ $\kappa_s^r = \kappa_s/(R\mu_0)$ and $\mu_s^r = \mu_s/(R\mu_0)$ are two-dimensional parameters, where the upper index r and lower index s denote radial and surface, respectively.¹¹ R denotes the radius of the nano-inclusion and $\kappa_s = 2(2\lambda_s + \mu_s)$, where λ_s and μ_s are the interface moduli.¹¹ More detailed descriptions of the interface moduli can be found in references.^{11,12} In addition, the fourth-rank Eshelby tensor for penny-shaped microcracks \mathbf{S}_2 is given in Lee and Pyo.¹³

The interface moduli represent the interfacial elasticity between spherical inhomogeneities and the matrix. The precise calculation and measurement of interfacial properties have been a contentious issue,¹⁴ and a full understanding of the interfaces of nanocomposites would be an enormous advancement.¹⁵ Therefore, the interfacial parameters are indirectly determined in the present study by comparing predictions based on the micromechanical model and the full atomistic MD simulation results. Since the full atomistic nature of heterogeneous materials can be ideally described by MD simulation, the proposed approach would be useful in reflecting the physical/mechanical nature of the interface. After carrying out the lengthy algebra, the fourth-rank tensor \mathbf{C}_* is proposed to be

$$\mathbf{C}_* = \lambda_{IK}^* \delta_{ij} \delta_{kl} + \mu_{IJ}^* (\delta_{ik} \delta_{jl} + \delta_{il} \delta_{jk}) \quad (6)$$

with

$$\lambda_{IK}^* = 2\lambda_0 \chi_{KK}^{(2)} + 2\mu_0 \chi_{IK}^{(1)} + \lambda_0 \sum_{n=1}^3 \chi_{nK}^{(1)}, \quad (7)$$

$$\mu_{IJ}^* = \mu_0 (\chi_{IJ}^{(2)} + \chi_{JI}^{(2)}),$$

where the parameters $\chi_{IK}^{(1)}$ and $\chi_{IJ}^{(2)}$ are given in the supplementary material.¹⁶ The nucleation of microcracks is

modeled in accordance with the continuum damage model.¹⁷ The volume fraction of nucleated microcracks in the composite is described by following an isotropic scalar function:¹⁷

$$\phi_2 = \begin{cases} \phi_{initial}, & \varepsilon^a \leq \varepsilon^{th} \\ \phi_{initial} + c_1 \left(1 - \frac{\varepsilon^{th}}{\varepsilon^a}\right)^{c_2}, & \varepsilon^a > \varepsilon^{th}, \end{cases} \quad (8)$$

where $\phi_{initial}$ is the initial volume fraction of microcracks, ε^{th} is the effective strain threshold below which no nucleation occurs, ε^a is the current accumulated effective strain, and c_1 and c_2 are nucleation parameters that depend on the specific shape and distribution of microcracks.¹⁷

To describe the interface effects on the micromechanical model, a series of numerical simulations are performed. The silica/nylon 6 nanocomposite system is chosen for the tests, and the parameters adopted for the nylon 6 matrix are $Y_0 = 2.8$ GPa and $\nu_0 = 0.34$; the parameters adopted for the silica NPs are $Y_1 = 73.1$ GPa, $\nu_1 = 0.17$, where Y_q and ν_q ($q = 0, 1$) denote the Young's modulus and Poisson's ratio of the q -phase, respectively.¹⁸ By varying the values of the interface moduli λ_s and μ_s , we then demonstrate the change in the bulk modulus (B_0) of the nanocomposite as a function of particle size (characterized as a radius R) and volume fraction (ϕ_1) in Fig. 1.

Fig. 1(a) shows that the bulk modulus becomes stiffer with a decrease in the NP size and an increase in the interface moduli, and it has a significant impact on the mechanical properties given the small length scale. However, the influence of the interfacial effects begins to diminish when the NP size exceeds 15 nm, until a state without interfacial effects is eventually reached. The predicted effective bulk modulus versus volume fraction of NPs is consistent with

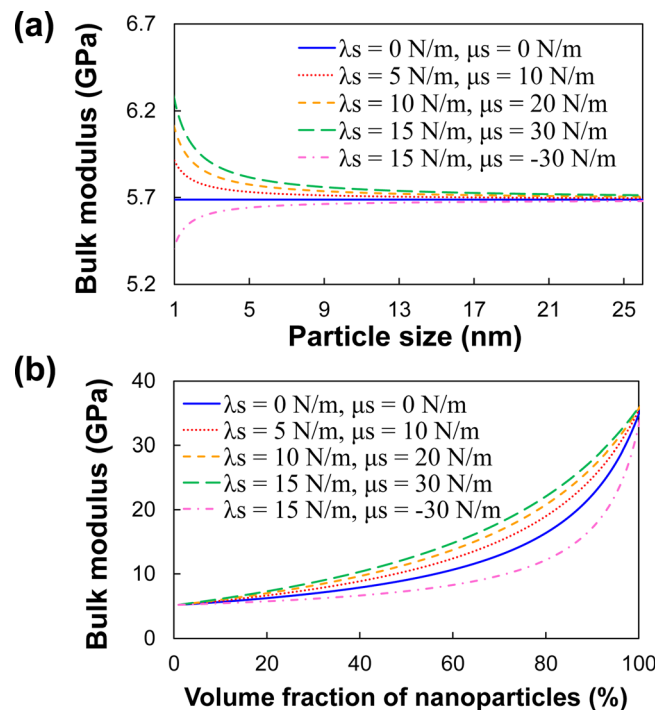


FIG. 1. The predicted bulk modulus of the nanocomposite versus (a) particle size and (b) content of NPs for different interface moduli.

previously reported simulations. It is important to note that the interfacial condition can yield negative effects on the mechanical response of nanocomposites. These effects are due to the imperfect interface between inclusions and the matrix,⁴ and such a tendency becomes more pronounced when the particle size decreases and the interfacial area increases.

To derive realistic values for the interface moduli λ_s and μ_s , we carry out atomistic MD simulations by using the Large-scale Atomistic Modeling Massively Parallelized Simulation (LAMMPS) code.¹⁹ The simulation cells of the nanocomposites consist of a single linear nylon 6 chain composed of 320 repeating unit monomers ($M_w = 36$ kDa) and spherical silica NPs with a radius varying from 3.35 Å (SiO₄H₄) to 6.62 Å (Si₁₇O₅₂H₃₆) to 10.05 Å (Si₈₃O₂₂₀H₁₀₈), as shown in Fig. 2(a). The interatomic potential is described using a DREIDING generic force field (FF),²⁰ and the partial charge distributions of the nylon 6 are determined as electrostatic potential (ESP) charges derived by Density functional theory (DFT) calculations at the M06-2X (Ref. 21)/6-31G** (Refs. 22 and 23) level for a hexanamide molecule, which represents the monomer of nylon 6 (-C₆H₁₁NO-). The partial charges of the silica NPs are determined by the charge equilibration (QEeq) method.²⁴ It should be noted that DFT calculations are performed using the Jaguar 7.6 software program.²⁵ The bulk moduli of the nanocomposites are then calculated as a function of the volume fraction and size of the silica NPs by fitting the equation of state (EoS) from MD simulation using the third-order Birch-Murnaghan (BM) equation,²⁶ as representatively shown in Fig. 2(b).

Since the dynamics of polymeric systems with long chains are slow, it is often troublesome to reach a well-equilibrated state within a finite MD simulation time scale. To overcome this obstacle and remove any possible bias originating from the choice of the initial polymer configuration, we use the MD procedure called the scaled effective solvent (SES) method, which was recently developed to efficiently obtain the equilibrium state of heterogeneous polymeric systems.²⁷ The mechanical properties of the nylon 6 matrix system with/without silica NPs obtained from MD simulations are listed in Table I. It is shown that embedding silica NPs into nylon 6 nanocomposites enhances the mechanical properties thereof, where the B_0 of the nanocomposites is enhanced with the radius of the silica NPs from 6.61

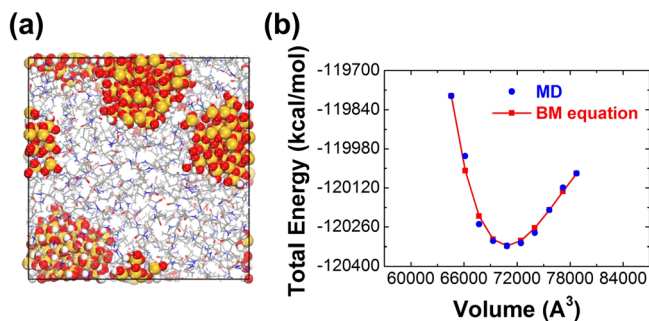


FIG. 2. (a) The final snapshot after the entire MD procedure and (b) the equation of states (EoS) of the nylon 6 nanocomposite with three silica NPs (Si₈₃O₂₂₀H₁₀₈). The white, red, orange, blue, and gray atoms are hydrogen, oxygen, silicon, nitrogen, and carbon atoms, respectively. The periodic box is indicated by a black solid line.

TABLE I. Mechanical properties of the nylon 6 matrix system with/without silica NPs obtained from MD simulations (R : radius of silica NPs, N_p : the number of NP in the simulation cell, ϕ_1 : volume fraction of NP, B_0 : bulk modulus of the system evaluated by BM EoS, ν_0 : Poisson's ratio).

System	R (Å)	N_p	ϕ_1 (%)	B_0 (GPa)	ν_0
w/o silica	6.61	0.34
w/SiO ₄ H ₄	3.35	6	1.62	6.95	-
w/Si ₁₇ O ₅₂ H ₃₆	6.62	6	11.28	7.01	-
w/Si ₈₃ O ₂₂₀ H ₁₀₈	10.05	6	30.78	8.37	-

to 8.37 GPa. Supplementary material regarding the MD simulations is available in the online version of the paper.¹⁶

Assuming that the interfacial conformation of the nanocomposites is identical for all samples so that the same values of the interface moduli are applicable to all cases regardless of the constituent properties, we find that $\lambda_s = 1.4$ N/m and $\mu_s = 1.0$ N/m leads to micromechanics results comparable to the MD simulation results (Fig. 3). The micromechanics-based constitutive model described above is then implemented in the FEM code ABAQUS to assess the predictive capability of the present framework. The C3D8 element in ABAQUS is used for the modeling, and the constitutive model of the nanocomposites is implemented by using a user-defined material routine within ABAQUS.

The material properties are sourced from the experimental data.^{18,28} These values are $Y_0 = 1.76$ GPa, $\nu_0 = 0.41$; $Y_1 = 73.1$ GPa, $\nu_1 = 0.17$, $R = 20$ nm, and $\phi_1 = 1\%$. The estimated interface moduli $\lambda_s = 1.4$ N/m and $\mu_s = 1.0$ N/m and the model parameters of the microcracks $\varepsilon^{th} = 0.01$, $c_1 = 0.5$ and $c_2 = 2.0$ are used in the comparison. The stress-strain curves of the experimental results²⁸ and of the present

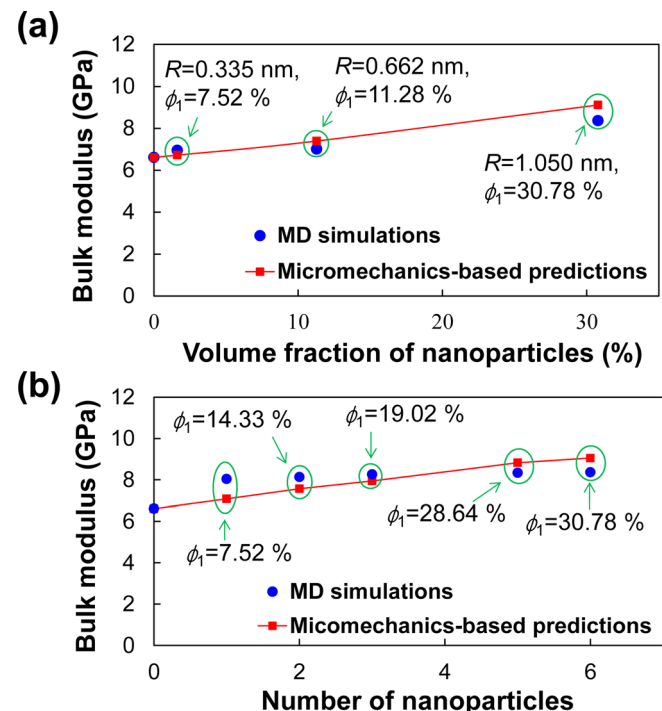


FIG. 3. Comparisons between the MD simulation and micromechanics-based predictions.

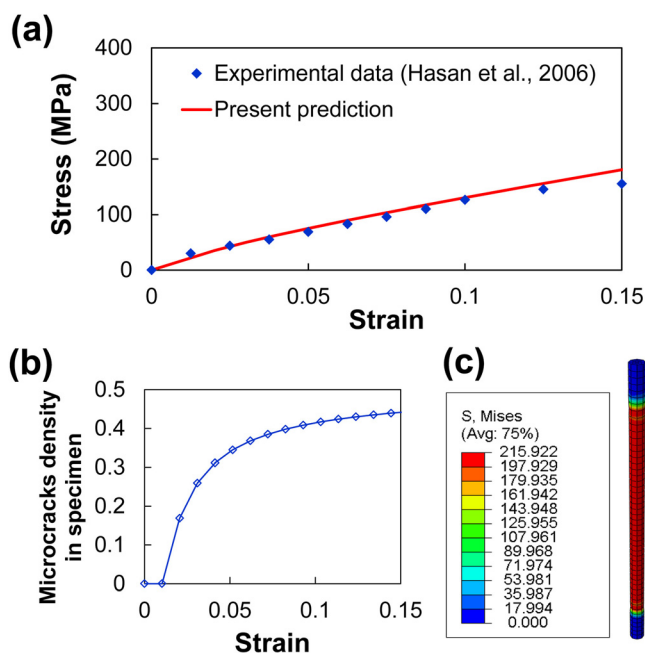


FIG. 4. (a) A comparison between the present prediction and the experimental data; (b) the evolution of the microcrack density; and (c) the deformed shape and von Mises stress distribution.

predictions are presented in Fig. 4. The predicted stress-strain curve and the experimental data show a good agreement up to the yielding point of the specimen, $\sigma_y = 129$ MPa, where the lower index y indicates the yield stress.²⁸ The observed divergence from the experiment at higher strain values is due to the intrinsic limitation of the present micromechanical model.

The proposed method, using the optimized parameters from the microscopic scale combined with macroscopic continuum theory and simulations, enables precise predictions on the mechanical behavior of large scale nanocomposite materials whose direct atomistic MD simulation is impractical. Unlike previous studies in which the aforementioned methods have been separately applied to predict the behavior of nanocomposites, the proposed methods offer a multiscale approach for efficient and extendable modeling. Although the different simulation techniques take different approaches, they are combined in the present study based on a developed micromechanical model that bridges MD simulation and FEM theory. To extend our theory to cover the prediction range into the higher strain regime, additional physical characteristics such as the yield strength and plastic behaviors should be taken into account. It is beyond the scope of the

present paper; however we plan to extend our work along this direction in the near future.

This research was sponsored by the National Research Foundation of Korea (NRF) Grants funded by the Korea Government (2013028443 and 2012M1A2A2026588) and the National Institute of Supercomputing and Networking/Korea Institute of Science and Technology Information with supercomputing resources including technical support (KSC-2012-C3-32). We also acknowledge the support by the Global Frontier R&D Program (2013-073298) on Center for Hybrid Interface Materials (HIM) funded by the Ministry of Science, ICT & Future Planning.

- ¹A. P. Meera, R. Tlili, A. Boudenne, L. Ibos, V. Poornima, S. Thomas, and Y. Candau, *J. Elastomers Plast.* **44**, 369 (2012).
- ²S. R. Chae, J. Moon, S. Yoon, S. Bae, P. Levitz, R. Winarski, and P. J. M. Monteiro, *Int. J. Concrete Struct. Mater.* **7**, 95 (2013).
- ³T. Laha, S. Kuchibhatla, S. Seal, W. Li, and A. Agarwal, *Acta Mater.* **55**, 1059 (2007).
- ⁴D. Ciprari, K. Jacob, and R. Tannenbaum, *Macromolecules* **39**, 6565 (2006).
- ⁵J. Jordan, K. I. Jacob, R. Tannenbaum, M. A. Sharaf, and I. Jasiuk, *Mater. Sci. Eng. A* **393**, 1 (2005).
- ⁶L. Zhu and K. A. Narh, *J. Polym. Sci. Part B: Polym. Phys.* **42**, 2391 (2004).
- ⁷B. J. Yang, B. R. Kim, and H. K. Lee, *Compos. Struct.* **94**, 1420 (2012).
- ⁸B. J. Yang, Y. Y. Hwang, and H. K. Lee, *Compos. Struct.* **99**, 123 (2013).
- ⁹H. K. Lee, *Comput. Mech.* **27**, 504 (2001).
- ¹⁰B. R. Kim, S. H. Pyo, G. Lemaire, and H. K. Lee, *Interact. Multiscale Mech.* **4**, 173 (2011).
- ¹¹H. L. Duan, H. T. Wang, Z. P. Huang, and B. L. Karihaloo, *Proc. R. Soc. A-Math. Phys.* **461**, 3335 (2005).
- ¹²D. J. Bottomley and T. Ogino, *Phys. Rev. B* **63**, 165412 (2001).
- ¹³H. K. Lee and S. H. Pyo, *J. Eng. Mech.* **135**, 1108 (2009).
- ¹⁴S. F. Ferdous, M. F. Sarker, and A. Adnan, *Polymer* **54**, 2565 (2013).
- ¹⁵J. Weissmuller and J. W. Cahn, *Acta Mater.* **45**, 1899 (1997).
- ¹⁶See supplementary material at <http://dx.doi.org/10.1063/1.4819383> for the process and results of MD simulations.
- ¹⁷Z. Liang, H. K. Lee, and W. Suaris, *Int. J. Solids. Struct.* **43**, 5674 (2006).
- ¹⁸G. W. C. Kaye and T. H. Laby, *Tables of Physical and Chemical Constants and Some Mathematical Functions* (Longman Scientific & Technical, New York, USA, 1995).
- ¹⁹S. Plimpton, *J. Comput. Phys.* **117**, 1 (1995).
- ²⁰S. L. Mayo, B. D. Olafson, and W. A. Goddard, *J. Phys. Chem.* **94**, 8897 (1990).
- ²¹Y. Zhao and D. G. Truhlar, *Theor. Chem. Acc.* **120**, 215 (2008).
- ²²W. J. Hehre, R. Ditchfield, and J. A. Pople, *J. Chem. Phys.* **56**, 2257 (1972).
- ²³P. C. Hariharan and J. A. Pople, *Theor. Chim. Acta* **28**, 213 (1973).
- ²⁴A. K. Rappe and W. A. Goddard, *J. Phys. Chem.* **95**, 3358 (1991).
- ²⁵Jaguar: Version 7.6, Schrödinger, LLC, New York, USA, 2009).
- ²⁶F. Birch, *Phys. Rev.* **71**, 809 (1947).
- ²⁷H. Shin, T. A. Pascal, W. A. Goddard, and H. Kim, *J. Phys. Chem. B* **117**, 916 (2013).
- ²⁸M. M. Hasan, Y. Zhou, H. Mahfuz, and S. Jeelani, *Mater. Sci. Eng. A* **429**, 181 (2006).